Journal of Organometallic Chemistry 693 (2008) 3281–3288

Contents lists available at ScienceDirect

Journal of Organometallic Chemistry

journal homepage: www.elsevier.com/locate/jorganchem

Interaction of *N*-(aryl)picolinamides with iridium. N–H and C–H bond activations

Moutusi Dasgupta [a], Haregewine Tadesse [b], Alexander J. Blake [b], Samaresh Bhattacharya [a,*]

[a] *Department of Chemistry, Inorganic Chemistry Section, Jadavpur University, Kolkata 700 032, India*
[b] *School of Chemistry, University of Nottingham, University Park, Nottingham NG72RD, UK*

ARTICLE INFO

Article history:
Received 18 May 2008
Received in revised form 18 July 2008
Accepted 22 July 2008
Available online 27 July 2008

Keywords:
N-(Aryl)picolinamides
Iridium
N–H and C–H bond activations

ABSTRACT

Reaction of *N*-(4-R-phenyl)picolinamide (R = OCH_3, CH_3, H, Cl and NO_2) with $[Ir(PPh_3)_3Cl]$ in refluxing ethanol in the presence of a base (NEt_3) affords two yellow complexes (**1-R** and **2-R**). The **1-R** complexes contain an amide ligand coordinated to the metal center as a monoanionic bidentate N,N donor along with two triphenylphosphines, a chloride and a hydride. The **2-R** complexes contain an amide ligand coordinated to the metal center as a monoanionic bidentate N,N donor along with two triphenylphosphines and two hydrides. Similar reaction of *N*-(naphthyl)picolinamide with $[Ir(PPh_3)_3Cl]$ affords two organometallic complexes, **3** and **4**. In complex **3** the amide ligand is coordinated to the metal center, via C–H activation of the naphthyl ring at the 8-position, as a dianionic tridentate N,N,C donor, along with two triphenylphosphines and one chloride. Complex **4** is similar to complex **3**, except a hydride is bonded to iridium instead of the chloride. Structures of the **1-OCH_3**, **2-Cl** and **4** complexes have been determined by X-ray crystallography. All the complexes are diamagnetic, and show characteristic ^1H NMR signals and intense MLCT transitions in the visible region. Cyclic voltammetry on all the complexes shows a Ir^{III}–Ir^{IV} oxidation within 0.50–1.16 V *vs.* SCE and a reduction of the coordinated amide ligand within −1.02 to −1.25 V *vs.* SCE.

1. Introduction

The chemistry of iridium has been receiving considerable current attention [1], largely because of the interesting properties exhibited by the complexes of this metal. As properties of the complexes are dictated primarily by the coordination environment around the metal center, complexation of iridium by ligands of selected types has been of significant importance, and the present work has originated from our interest in this area [2]. Herein we have selected a group of amide ligands (**L^1**) derived from picolinic acid and *para*-substituted anilines. The selected amide ligands (**L^1**) are known to bind to metal ions usually as neutral N,O-donor (amide form, **I**) or monoanionic N,N-donor (amidate form, **II**) via loss of the amide proton [3]. A third mode of chelation, as monoanionic N,O-donor (**III**), has also been observed by us [4]. Chemistry of the amide ligands is of particular interest with reference to their role in biological processes [5]. For example, the amide linkage plays a key role in the formation and maintenance of protein architectures, which are crucial for their performance in biological systems [6]. Chelation in the amidate mode (**II**) is known to stabilize metal ions in their higher oxidation states, while that in the amide mode (**I**) is reported to favor relatively lower oxidation states of a metal [3]. Interconversion between the amide (**I**) and amidate (**II**) modes of binding has been utilized to chemically manipulate redox properties of the metal center [7]. It may be mentioned here that though the chemistry of amide complexes of many transition metals has been extensively studied [8], that of iridium appears to have received much less attention [9]. As the source of iridium the $[Ir(PPh_3)_3Cl]$ complex has been chosen, because of its demonstrated ability to undergo facile reaction with ligands having dissociable protons affording stable mixed-ligand hexacoordinated complexes [2]. Reaction of the selected amides (**L^1**) as well as a related ligand, *viz.* *N*-(naphthyl)picolinamide (**L^2**), with $[Ir(PPh_3)_3Cl]$ has been found to afford interesting complexes, where the amides (**L^1** and **L^2**) are bound to the metal center as in **II** and **IV**, respectively. The chemistry of all these complexes is reported here, with special reference to their formation, characterization and, spectral and electrochemical properties.

* Corresponding author.
E-mail address: samaresh_b@hotmail.com (S. Bhattacharya).

0022-328X/$ - see front matter © 2008 Elsevier B.V. All rights reserved.
doi:10.1016/j.jorganchem.2008.07.027

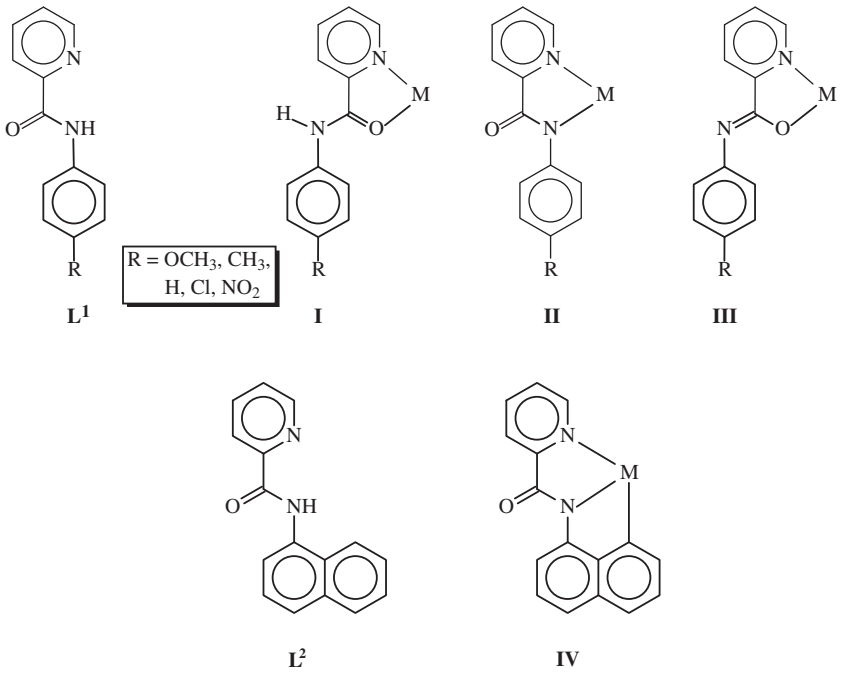

2. Results and discussion

2.1. Synthesis and characterization

As delineated in the introduction, the primary objectives of the present study have been to study the interaction of the selected *N*-(4-R-phenyl)picolinamides (**L**[1]) with iridium and see how they bind to the metal center. The five different substituents, with different electron withdrawing properties, have been chosen to study their influence, if any, on the redox properties of the resulting complexes. Reaction of these amides (**L**[1]) with [Ir(PPh$_3$)$_3$Cl] proceeds smoothly in refluxing ethanol in the presence of triethylamine. From each of these reactions two yellow complexes (**1-R** and **2-R**) have been obtained in comparable and decent yields. Preliminary characterizations (microanalysis, IR, NMR, etc.) on the **1-R** complexes indicate presence of an amide ligand, a chloride, a hydride and two triphenylphosphines in the coordination sphere. In the **2-R** complexes, however, it has been found that along with a coordinated amide ligand, two triphenylphosphines and two hydrides are also present.

In order to find out stereochemistry of these complexes, as well as to ascertain coordination mode of the amide ligand in them, structure of a representative member from both the series, *viz.* **1-OCH$_3$** and **2-Cl**, has been determined by X-ray crystallography. Structure of the **1-OCH$_3$** complex is shown in Fig. 1 and some relevant bond parameters are listed in Table 2. The structure shows that the *N*-(4-methoxyphenyl)picolinamide is coordinated to iridium, via dissociation of the amide proton, as a bidentate N,N-donor forming a five-membered chelate ring (**II**). Two triphenylphosphines, a chloride and a hydride are also coordinated to the metal center. The coordinated picolinamide, hydride and chloride have constituted an equatorial plane with the metal at the center, where the chloride is *trans* to the amide nitrogen and the hydride is *trans* to the pyridine nitrogen. The two PPh$_3$ ligands have occupied the remaining two axial positions and hence they are mutually *trans*. The Ir–H1, Ir–N1, Ir–P1, Ir–P2 and Ir–Cl1 distances are quite normal [2], and so are the distances within the chelated amide ligand [3,8]. However, the Ir–N4 bond is noticeably longer than the Ir–N1 bond. The observed elongation of the Ir–N4 bond is thus attributable to the *trans* effect of the coordinated hydride (H1). The absence of any solvent of crystallization in the lattice of **1-OCH$_3$** indicates possible existence of non-covalent interaction(s) between the individual complex molecules. A closer look at the packing pattern of the crystal (shown in Fig. 2) reveals that C–H···O and C–H···π interactions, involving phenyl C–H, are active in the lattice. Each complex molecule is thus linked with the surrounding complex molecules through these hydrogen-bonding interactions, and these extended intermolecular interactions seem to be responsible for holding the crystal together. It may be relevant to note here that such non-covalent interactions are of significant importance in crystal engineering and biology [10]. As all the **1-R** complexes have been synthesized similarly and they show similar properties (*vide infra*), the other four **1-R** ($R \neq OCH_3$) complexes are assumed to have similar structures as the **1-OCH$_3$** complex.

Structure of the **2-Cl** complex (shown in Fig. 3) is found to be qualitatively similar to that of the **1-OCH$_3$** complex, except that a second hydride is coordinated to iridium *trans* to the pyridine ring in the former instead of the chloride in the latter. While most of the bond distances (Table 2) are comparable to those observed in the earlier structure, the Ir–N2 length is significantly longer in this complex compared to that in the **1-OCH$_3$** complex, which is attributable, as before, to the *trans* effect of the second hydride (H2). To find out the nature of intermolecular interactions in the lattice of **2-Cl**, its packing pattern has been examined, which shows that C–H···Cl, C–Cl···π and C–H···π interactions are active (*Fig.* S1, Supplementary material) and they link the individual complex molecules to form a stable lattice. As all the five complexes in this series have been synthesized similarly and they show similar properties (*vide infra*), the other four ($R \neq Cl$) complexes are assumed to have similar structures as the **2-Cl** complex.

Formation of the **1-R** and **2-R** complexes, containing one and two coordinated hydrides, respectively, from the same synthetic reaction has been quite interesting. While the exact sequences behind formation of these two types of complexes are not exactly clear to us, the speculated steps illustrated in Scheme 1 seem probable. In the initial step the amide ligand (**L**[1]) interacts with the metal center in [Ir(PPh$_3$)$_3$Cl], whereby oxidative insertion of iridium into the N–H bond of the amide ligand takes place associated with the simultaneous loss of a PPh$_3$ from the iridium starting material, and thus complex **1-R** is formed. Precedence of such bond

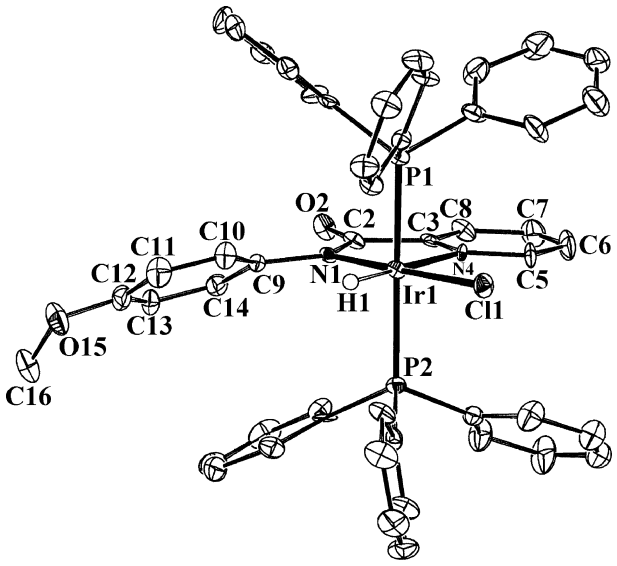

Fig. 1. View of the **1-OCH$_3$** complex.

Table 1
Crystallographic data for **1-OCH$_3$**, **2-Cl** and **4** complexes

	Complex **1-OCH$_3$**	Complex **2-Cl**	Complex **4**
Empirical formula	$C_{49}H_{42}N_2O_2ClP_2Ir$	$C_{48}H_{40}N_2OClP_2Ir$	$C_{52}H_{41}N_2OP_2Ir$
Fw	980.44	950.41	964.01
Crystal system	Orthorhombic	Monoclinic	Monoclinic
Space group	*Pna*2$_1$	*P*2$_1$/*c*	*Cc*
a (Å)	35.583(11)	12.1755(7)	11.3149(8)
b (Å)	9.790(3)	24.2409(15)	21.7520(15)
c (Å)	11.552(4)	14.3847(9)	17.5661(12)
α (°)	90	90	90
β (°)	90	110.432(2)	108.4980(10)
γ (°)	90	90	90
V (Å^3)	4042(2)	3978.5(4)	4100.0(5)
Z	4	4	4
λ (Å)	0.71073	0.71073	0.71073
F (000)	1956	1888	1924
Crystal size (mm)	0.02 × 0.05 × 1.50	0.09 × 0.16 × 0.54	0.05 × 0.12 × 0.22
T (K)	150	150	150
μ (mm^{-1})	3.508	3.544	3.377
R_1[a]	0.0323	0.0273	0.0238
wR_2[b]	0.0647	0.0686	0.0530
GOF[c]	1.08	1.03	1.08

[a] $R_1 = \sum||F_o| - |F_c||/\sum|F_o|$.
[b] $wR_2 = [\sum[w(F_o^2 - F_c^2)^2]/\sum[w(F_o^2)^2]]^{1/2}$.
[c] GOF = $[\sum[w(F_o^2 - F_c^2)^2]/(M - N)]^{1/2}$, where *M* is the number of reflections and *N* is the number of parameters refined.

Table 2
Selected bond lengths (Å) and bond angels (°) for the **1-OCH$_3$**, **2-Cl** and **4** complexes

Complex **1-OCH$_3$**			
Bond distances (Å)			
Ir(1)–Cl(1)	2.3990(17)	C(2)–O(2)	1.246(6)
Ir(1)–P(1)	2.3331(14)	C(2)–N(1)	1.363(6)
Ir(1)–P(2)	2.3117(13)	C(9)–N(1)	1.436(6)
Ir(1)–N(1)	2.077(4)		
Ir(1)–N(4)	2.144(5)		
Bond angles (°)			
P(1)–Ir(1)–P(2)	172.51(9)	N(1)–Ir(1)–N(4)	78.26(16)
N(1)–Ir(1)–Cl(1)	174.65(11)		
Complex **2-Cl**			
Bond distances (Å)			
Ir(1)–P(1)	2.2890(8)	C3–O1	1.246(4)
Ir(1)–P(2)	2.3046(8)	C3–N2	1.338(4)
Ir(1)–N(2)	2.179(3)	C10–N2	1.423(4)
Ir(1)–N5	2.136(2)		
Bond angles (°)			
P(1)–Ir(1)–P(2)	165.72(3)	N(2)–Ir(1)–N(5)	76.78(9)
Complex **4**			
Bond distances (Å)			
Ir(1)–P(1)	2.3124(11)	C(3)–O(1)	1.241(4)
Ir(1)–P(2)	2.3010(11)	C(3)–N(1)	1.348(5)
Ir(1)–C(10)	2.041(4)	C(18)–N(1)	1.409(5)
Ir(1)–N(1)	2.068(3)		
Ir(1)–N(5)	2.135(3)		
Bond angles (°)			
P(1)–Ir(1)–P(2)	172.72(4)	C(10)–Ir(1)–N(1)	81.54(12)
C(10)–Ir(1)–N(5)	159.84(12)	N(1)–Ir(1)–N(5)	78.33(11)

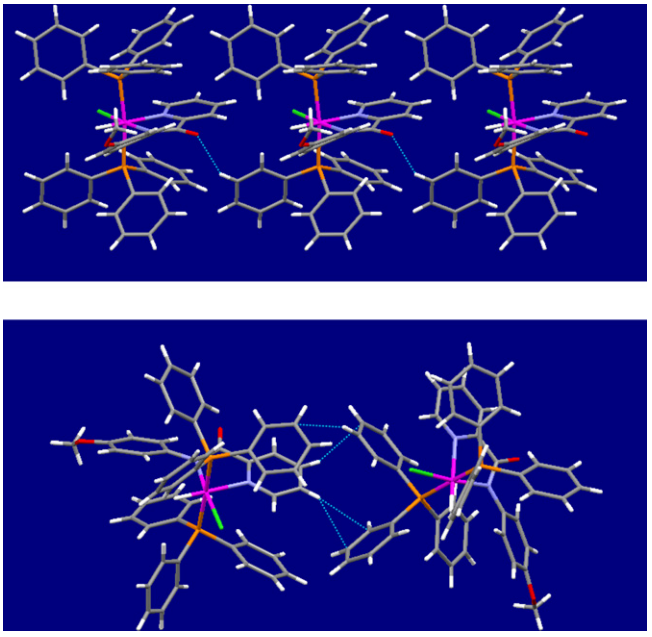

Fig. 2. C–H···O (top) and C–H···π (bottom) interactions in the lattice of the **1-OCH$_3$** complex.

activation by iridium(I) forming hydride complex of iridium(III) has been observed before [2]. In the next step the Ir–Cl bond in the **1-R** complex reacts with ethanol in the presence of NEt$_3$, whereby it is converted into an Ir–H bond and thus complex **2-R** is produced. Such conversion of M–Cl into M–H in alcoholic medium is well documented in the literature [11]. Evidence for this transformation comes from the fact that ethanolic solution of any **1-R** complex is observed to slowly convert into the corresponding **2-R** complex in the presence of NEt$_3$ [12]. Therefore, source of the hydride in **1-R** complex is the N–H fragment of the amide ligand and that of the second hydride in **2-R** complex is the solvent (ethanol). It is relevant to mention in this context that when reaction of the amide ligands (**L^1**) with [Ir(PPh$_3$)$_3$Cl] is carried out in a nonalcoholic solvent (*viz.* toluene) in the presence of triethylamine, only the **1-R** complexes are obtained, which also supports our conclusion stated above regarding origin of hydride(s) in the **1-R** and **2-R** complexes.

Disposition of the Ir–H bond, which is *trans* to the pyridine nitrogen, with respect to the pendent phenyl ring in both the **1-R** and **2-R** complexes points to the possibility of a C–H activation of the aryl ring. However, such an activation could not take place in the **1-R** or **2-R** complexes, because in them the phenyl ring is not close enough to the metal center and had the phenyl ring undergone an orthometallation, it would have resulted in the

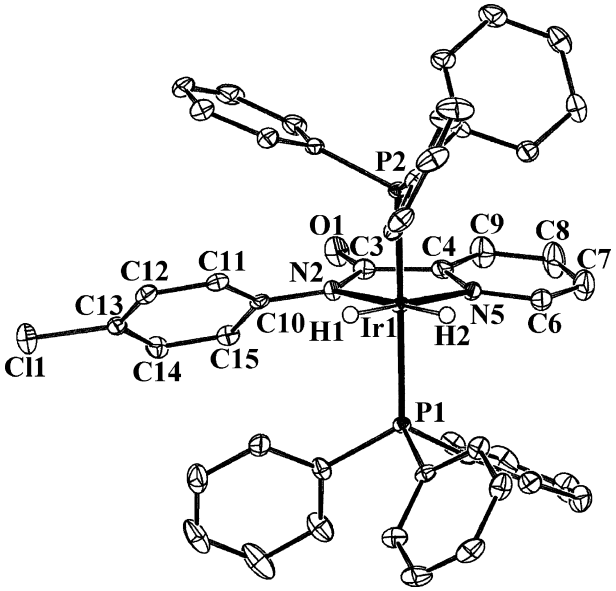

Fig. 3. View of the **2-Cl** complex.

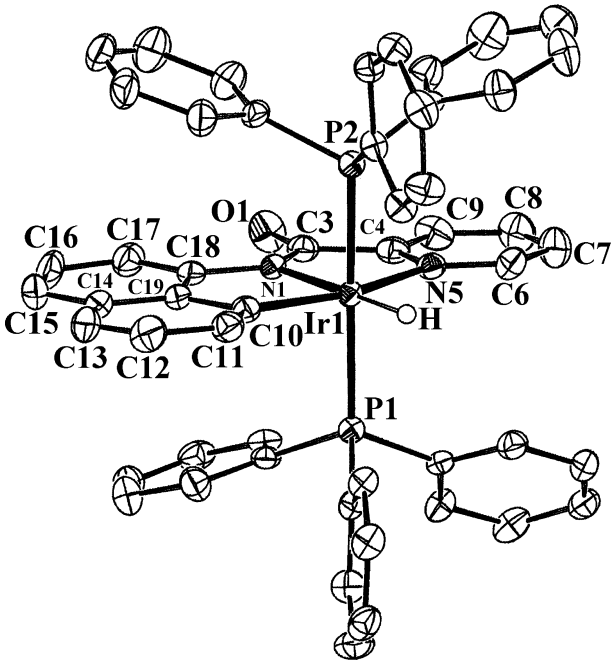

Fig. 4. View of complex **4**.

formation of a sterically unstable four-membered metallacycle. In order to induce a facile C–H activation the aryl fragment needs to be so chosen that one of its C–H bond should come in close proximity to the Ir–H bond. With this simple strategy in mind, a new amide ligand, *viz*. *N*-(naphthyl)picolinamide (**L²**); where a naphthyl ring has replaced the phenyl ring in **L¹**, has been chosen as the target ligand for the C–H activation. Reaction of *N*-(naphthyl)picolinamide with $[Ir(PPh_3)_3Cl]$ has been carried out similarly as before, which has afforded two orange complexes (**3** and **4**). While yield of complex **3** is low, that of complex **4** is good. Preliminary characterizations on complex **3** indicate the presence of an amide ligand, two triphenylphosphines and a chloride in the coordination sphere. Composition of complex **4** has been found to be similar to that of complex **3**, except a hydride is coordinated to iridium instead of the chloride. Structural characterization of complex **3** has not been possible, as its crystals could not be grown. However, it has been assumed to have a similar (hydride replaced by chloride) structure as complex **4**. Structure of complex **4** has been determined by X-ray crystallography. The structure (shown in Fig. 4) shows that the *N*-(naphthyl)picolinamide is indeed coordinated to iridium in the expected N,N,C-fashion (**IV**). A hydride is coordinated *trans* to the amide nitrogen, and two triphenylphosphines are occupying the axial positions. The Ir–C distance is normal [2], and the other bond distances are comparable to those in the previous complexes (Table 2). An examination of the packing pattern of complex **4** shows that C–H···O and C–H···π interactions are active (*Fig.* S2, Supplementary material) in the lattice.

The speculated sequences behind formation of the two organoiridium complexes (**3** and **4**) from the same synthetic reaction are shown in Scheme 2. As shown earlier in Scheme 1, the N–H fragment of the amide ligand (**L²**) is believed to add oxidatively to the metal center in $[Ir(PPh_3)_3Cl]$ generating a hydride intermediate (**A**), which is gradually converted into a dihydride derivative (**B**). These intermediates then undergo cyclometallation via elimination of molecular hydrogen affording the organoiridium complexes (**3** and **4**) [13]. It is relevant to mention here that when similar reaction of the amide ligand (**L²**) with $[Ir(PPh_3)_3Cl]$ is carried out in toluene, complex **3** is obtained as the sole product. This demonstrates that, as described before, in the absence of alcoholic solvent the dihydride intermediate **B** is not formed and thus complex **4** is not obtained.

2.2. Spectral studies

Magnetic susceptibility measurements show that all the iridium complexes are diamagnetic, which corresponds to the +3 oxidation state of iridium (low-spin d^6, $S = 0$) in these complexes. ^1H NMR spectra of the **1-R** complexes show broad signals within 7.09–7.61 ppm for the coordinated PPh_3 ligands. The hydride signal is

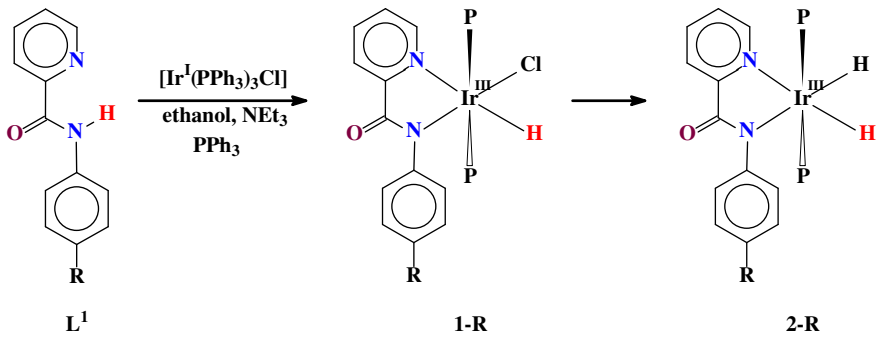

Scheme 1. Probable steps for the formation of the **1-R** and **2-R** complexes.

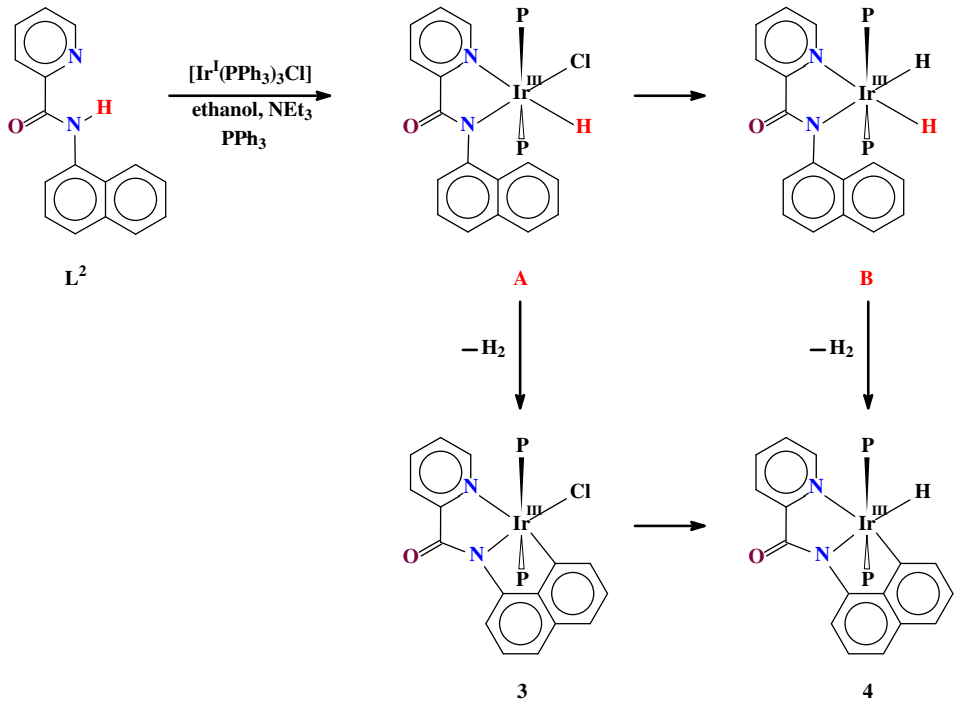

Scheme 2. Probable steps for the formation of complexes **3** and **4**.

Table 3
Electronic spectral and cyclic voltammetric data of the complexes

Compound	Electronic spectral data[a] λ_{max}, nm (ε, M^{-1} cm^{-1})	Cyclic voltammetric data[b] E/V *vs.* SCE
1-OCH$_3$	413 (3500), 278[c] (17650), 239 (35100)	0.78[d](75)[e], −1.12[f]
1-CH$_3$	416 (3300), 270[c] (17200), 232 (34900)	0.78[d](76)[e], −1.18[f]
1-H	414 (3300), 276[c] (18300), 238 (33300)	1.01[d](93)[e], −1.12[f]
1-Cl	414 (3000), 272[c] (18900), 236 (33000)	1.03[d](87)[e], −1.08[f]
1-NO$_2$	437 (9400), 298[c] (11800), 270 (17400), 234 (35900)	1.16[d](98)[e], −1.17[f]
2-OCH$_3$	417 (4400), 359[c] (5500), 333 (8100), 267[c] (24600), 243 (35300)	0.74[g], −1.13[f]
2-CH$_3$	414 (3900), 359[c] (5000), 335 (7900), 274[c] (19400), 243 (33100)	0.68[g], −1.02[f]
2-H	407 (3300), 350[c] (4700), 333 (6500), 265[c] (1900), 243 (28800)	0.80[g], −1.12[f]
2-Cl	413 (4100), 346[c] (6400), 329 (8400), 265[c] (22800), 242 (32400)	0.78[g], −1.25[f]
2-NO$_2$	434 (17700), 339[c] (10100), 325(13200), 270[c] (22600), 244 (36800)	0.93[g], −1.16[f]
3	478 (3400), 393[c] (5200), 349 (9300), 283 (13300), 296[c] (12000), 239 (35900)	0.50[g], −1.23[f]
4	489 (2900), 391[c] (5300), 346 (9200), 302 (10900), 285[c] (12200), 242 (34100)	0.51[g], −1.22[f]

[a] In dichloromethane.
[b] Solvent, 1:9 dichloromethane–acetonitrile; supporting electrolyte, TBAP; scan rate, 50 mV s^{-1}.
[c] Shoulder.
[d] $E_{1/2} = 0.5(E_{pa} + E_{pc})$, where E_{pa} and E_{pc} are anodic and cathodic peak potentials, respectively.
[e] $\Delta E_p = E_{pa} - E_{pc}$.
[f] E_{pc} value.
[g] E_{pa} value.

observed around −17.1 ppm. Signals for the methoxy and methyl groups in the **1-OCH$_3$** and **1-CH$_3$** complexes are observed, respectively, at 3.63 and 2.08 ppm. Most of the expected aromatic proton signals from the coordinated amide ligand are clearly observed in the expected region, while a few could not be detected due to their overlap with other signals in the same region. In the ^{1}H NMR spectra of the **2-R** complexes two distinct hydride signals are observed near −19.3 and −20.4 ppm. Besides small shifts in the signal positions, rest of the ^{1}H NMR spectrum of each **2-R** complex is qualitatively similar to that of the corresponding **1-R** complex. ^{1}H NMR spectrum of complex **3** is mostly similar to that of the **1-H** complex. Besides the hydride signal at −14.48 ppm, ^{1}H NMR spectrum of complex **4** is similar to that of complex **3**.

Infrared spectrum each **1-R** complex shows many bands of different intensities in the 400–4000 cm^{-1} region. No attempt has been made to assign each individual band to a specific vibration. However, comparison with the spectra of the corresponding uncoordinated ligands shows that the N–H stretch, observed near 3140 cm^{-1} in the uncoordinated ligand, is absent in the complexes. The amide C=O stretch, observed at around 1680 cm^{-1} in the uncoordinated ligand, is also found to be shifted to around 1579 cm^{-1} in the **1-R** complexes. A strong band displayed near 2181 cm^{-1} by the **1-R** complexes is due to the coordinated hydride. Three strong bands have been observed near 517, 692 and 746 cm^{-1} in **1-R** complexes indicating the presence of coordinated PPh_3 ligands [2]. Several sharp bands (*e.g.* near 823, 1093, 1178, 1245, 1346, 1434 and 1502 cm^{-1}) are also observed in the **1-R** complexes, which were absent in the $[Ir(PPh_3)_3Cl]$ complex, and hence these are attributed to the coordinated amide ligand. In the infrared spectra of the **2-R** complexes two distinct Ir–H stretches are observed near 2148 and 2120 cm^{-1}, and the rest of the spectra are similar to those of the **1-R** complexes. Infrared spectra of complexes **3** and **4** are also similar to those of the earlier complexes, where only complex **4** shows a Ir–H stretch at 2082 cm^{-1}.

The **1-R** and **2-R** complexes are soluble in acetone, dichloromethane, chloroform, acetonitrile, etc., producing bright yellow solutions. Complexes **3** and **4** also have similar solubility and produce orange solutions. Electronic spectra of all the complexes have been recorded in dichloromethane solution. Spectral data are presented in Table 3. All the complexes show several intense absorptions in the visible and ultraviolet regions. The absorptions in the ultraviolet region are attributable to transitions within the ligand orbitals, while those in the visible region are probably due to charge-transfer transitions. To have a better insight into the nature

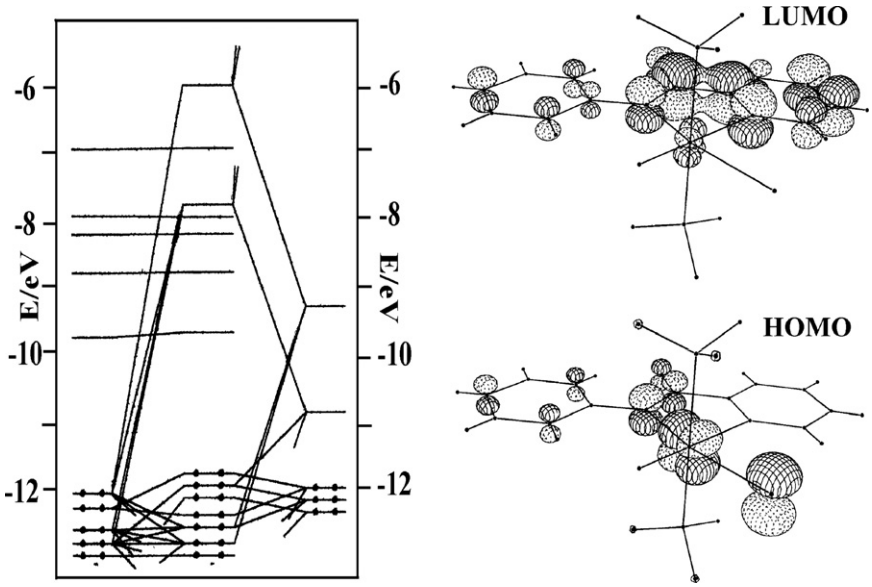

Fig. 5. Partial molecular orbital diagram of the **1-H** complex.

of absorptions in the visible region, qualitative EHMO calculations have been performed [14] on computer-generated models of the complexes. Partial MO diagrams for four selected complexes are shown in Fig. 5 and *Figs.* S3–S5 (Supplementary material) and the composition of selected molecular orbitals is given in *Table* S1 (Supplementary material). In the **1-R** complexes, the highest occupied molecular orbital (HOMO) and the next two filled orbitals (HOMO-1 and HOMO-2) have major (≥55%) contribution from the iridium d-orbitals. The lowest unoccupied molecular orbital (LUMO) is delocalized primarily on the amide ligand, and is concentrated mostly on the pyridyl ring and the amide fragment [15]. The next couple of vacant orbitals (*e.g.* LUMO + 1 and LUMO + 2) are also concentrated on the amide ligand. The intense absorption displayed by the **1-R** complexes near 410 nm may therefore be assigned to a charge-transfer transition taking place from the filled iridium d-orbital (HOMO) to the vacant π^*-orbital of the amide ligand (LUMO). In the **2-R**, **3** and **4** complexes, nature of the frontier molecular orbitals is very similar to that of the **1-R** complexes. Hence the lowest energy absorption in the **2-R**, **3** and **4** complexes are assignable to the HOMO-to-LUMO charge-transfer transition.

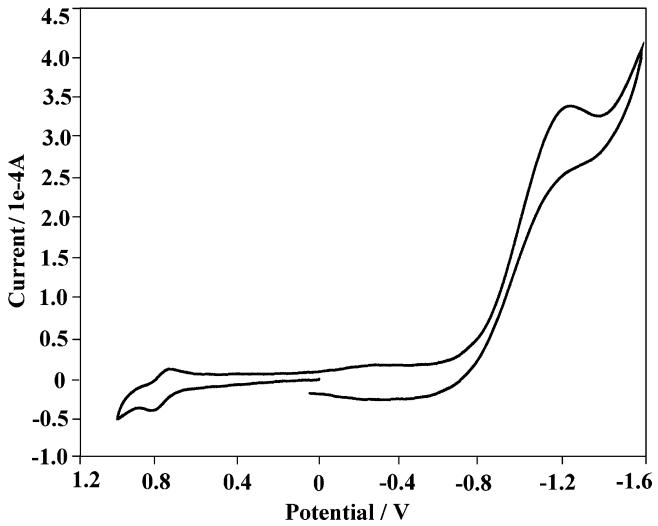

Fig. 6. Cyclic voltammogram of the **1-CH$_3$** complex in 1:9 dichloromethane–acetonitrile solution (0.1 M TBAP) at a scan rate of 50 mV s^{-1}.

2.3. Electrochemical properties

Electrochemical properties of the iridium complexes have been studied by cyclic voltammetry in 1:9 dichloromethane–acetonitrile solution (0.1 M TBAP) [16]. Voltammetric data are given in Table 3 and a selected voltammogram is shown in Fig. 6.

Each complex shows an oxidative response on the positive side of SCE and a reductive response on the negative side. In the **1-R** complexes the oxidative response is quasi-reversible in nature, and in view of composition of the HOMO in all these complexes, this is assigned to Ir^{III}–Ir^{IV} oxidation. One-electron nature of this oxidation has been confirmed by comparing its current height (i_{pa}) with that of standard ferrocene–ferrocenium couple under identical experimental conditions. In the other complexes (**2-R**, **3** and **4**) the Ir^{III}–Ir^{IV} oxidation appears as an irreversible response. The reductive response is irreversible in nature in all the complexes, and shows non-stoichiometric current (i_{pc}). Based on composition of the LUMO, the reduction is assigned to reduction of the coordinated amide ligand. Potential of the redox responses in the **1-R** and **2-R** complexes does not show any systematic variation with the nature of the substituent R.

3. Conclusions

The present study shows that upon reaction with $[Ir(PPh_3)_3Cl]$ the *N*-(aryl)picolinamides (**L^1**) can readily bind to iridium as monoanionic N,N-donors, whereby iridium oxidatively inserts into the amide N–H bond and thus generates an Ir–H bond. This study also demonstrates that the Ir–H bond can be utilized for inducing C–H activation of selective amides, such as *N*-(naphthyl)picolinamide.

4. Experimental

Iridium trichloride was purchased from Arora Matthey, Kolkata, India. Triphenylphosphine, the *para*-substituted anilines and 2-picolinic acid were purchased from S.D. Fine-Chem Limited, India.

All other chemicals and solvents were reagent grade commercial materials and were used as received. [Ir(PPh$_3$)$_3$Cl] was prepared by following a reported method. The *N*-(aryl)picolinamides were prepared by condensing picolinic acid with *para*-substituted anilines or α-naphthylamine [17] Purification of dichloromethane and acetonitrile, and preparation of tetrabutylammonium perchlorate (TBAP) for electrochemical work were performed as reported in the literature [18]. Microanalyses (C, H, N) were performed using a Heraeus Carlo Erba 1108 elemental analyzer. IR spectra were obtained on a Perkin–Elmer 783 spectrometer with samples prepared as KBr pellets. Electronic spectra were recorded on a JASCO V-570 spectrophotometer. ^{1}H NMR spectra were recorded in $CDCl_3$ solution with a Bruker Avance DPX 300 NMR spectrometer using TMS as the internal standard. Electrochemical measurements were made using a CH Instruments model 600A electrochemical analyzer. A platinum disc working electrode, a platinum wire auxiliary electrode and an aqueous saturated calomel reference electrode (SCE) were used in the cyclic voltammetry experiments. All electrochemical experiments were performed under a dinitrogen atmosphere. All electrochemical data were collected at 298 K and are uncorrected for junction potentials.

4.1. Synthesis of complexes

Complexes **1-OCH$_3$** and **2-OCH$_3$**: *N*-(4-methoxyphenyl)picolinamide (**L^1**, R = OCH_3) (23 mg, 0.10 mmol) was dissolved in warm ethanol (40 mL) and to it was added triethylamine (10 mg, 0.10 mmol), followed by [Ir(PPh$_3$)$_3$Cl] (100 mg, 0.10 mmol). The mixture was then refluxed for 24 h to yield a yellow solution. The solvent was evaporated and the solid mass, thus obtained, was subjected to purification by thin layer chromatography on a silica plate. With 1:5 acetonitrile/benzene as the eluant, two yellow bands separated, which were extracted with acetonitrile. Evaporation of these acetonitrile extracts gave **1-OCH$_3$** and **2-OCH$_3$** as yellow crystalline solids.

The other **1-R** and **2-R** (R ≠ OCH_3) complexes were prepared by following similar procedure as above using the respective amide ligands (**L^1**, R ≠ OCH_3).

Complex **1-OCH$_3$**: Yield: (34 mg, 35%); Anal. Calc. for $C_{49}H_{42}N_2O_2ClP_2Ir$: C, 60.01; H, 4.28; N, 2.85. Found: C, 60.13; H, 4.32; N, 2.83%. ^{1}H NMR [19]: −17.07 (t, hydride, *J* = 14.1 Hz); 3.63 (OCH_3); 6.08 (d, 2H, *J* = 9.0 Hz); 6.67 (t, H, *J* = 6.2 Hz); 6.86 (d, 2H, *J* = 9.0 Hz); 7.13–7.61 (2PPh$_3$); 7.66 (t, H, *J* = 5.9 Hz); 7.84 (d, H, *J* = 7.7 Hz); 8.13 (d, H, *J* = 5.1 Hz). Complex **1-CH$_3$**: Yield: (34 mg, 36%); Anal. Calc. for $C_{49}H_{42}N_2OClP_2Ir$: C, 61.01; H, 4.35; N, 2.90. Found: C, 60.59; H, 4.34; N, 2.93%. ^{1}H NMR: −17.10 (t, hydride, *J* = 14.1 Hz); 2.08 (CH_3); 6.31 (d, 2H, *J* = 8.3 Hz); 6.67 (t, 1H, *J* = 6.3 Hz); 6.75 (d, 2H, *J* = 8.3 Hz); 7.12–7.56 (2PPh$_3$); 7.54 (t, H, *J* = 7.6 Hz); 7.83 (d, H, *J* = 7.8 Hz); 8.11 (d, H, *J* = 5.1 Hz). Complex **1-H**: Yield: (30 mg, 32%); Anal. Calc. for $C_{48}H_{40}N_2OClP_2Ir$: C, 60.64; H, 4.21; N, 2.94. Found: C, 60.34; H, 4.20; N, 2.97%. ^{1}H NMR: −17.04 (t, hydride, *J* = 14.0 Hz); 6.52 (t, 1H, *J* = 7.1 Hz); 6.69 (t, 2H, *J* = 6.3 Hz); 6.96 (d, H, *J* = 7.1 Hz); 7.10–7.44 (2PPh$_3$); 7.55 (t, H, *J* = 7.7 Hz); 7.87 (d, H, *J* = 7.7 Hz); 8.13 (d, H, *J* = 5.1 Hz). Complex **1-Cl**: Yield: (33 mg, 34%); Anal. Calc. for $C_{48}H_{39}N_2OCl_2P_2Ir$: C, 58.52; H, 3.96; N, 2.84. Found: C, 58.67; H, 3.96; N, 2.81%. ^{1}H NMR: −17.10 (t, hydride, *J* = 14.1 Hz); 6.45 (d, 2H, *J* = 8.8 Hz); 6.70 (t, 1H, *J* = 6.3 Hz); 6.91 (d, 2H, *J* = 8.8 Hz); 7.14–7.54 (2PPh$_3$); 7.56 (t, H, *J* = 7.6 Hz); 7.85 (d, H, *J* = 7.7 Hz); 8.16 (d, H, *J* = 5.0 Hz). Complex **1-NO$_2$**: Yield: (34 mg, 35%); Anal. Calc. for $C_{48}H_{39}N_3O_3ClP_2Ir$: C, 57.90; H, 3.92; N, 4.22. Found: C, 57.69; H, 3.90; N, 4.25%. ^{1}H NMR: −17.03 (t, hydride, *J* = 14.1 Hz); 6.81 (t, H, *J* = 6.5 Hz); 6.94 (4H)*; 7.09–7.47 (2PPh$_3$); 7.62 (t, H, *J* = 7.5 Hz); 7.90 (d, H, *J* = 7.6 Hz); 8.28 (d, H, *J* = 5.2 Hz).

Complex **2-OCH$_3$**: Yield: (36 mg, 38%); Anal. Calc. for $C_{49}H_{43}N_2O_2P_2Ir$: C, 62.20; H, 4.54; N, 2.96. Found: C, 62.31; H, 4.50; N, 3.01%. ^{1}H NMR: −19.42 (d of t, hydride, J_d = 6.6 Hz, J_t = 6.6 Hz); −20.20 (d of t, hydride, J_d = 6.6 Hz, J_t = 6.9 Hz); 3.68 (OCH_3); 6.24 (d, 2H, *J* = 8.9 Hz); 6.32 (t, H, *J* = 6.4 Hz); 6.85 (d, 2H, *J* = 8.9 Hz); 7.12–7.46 (2PPh$_3$); 7.54 (d, H, *J* = 5.0 Hz); 7.73 (2H)*. Complex **2-CH$_3$**: Yield: (33 mg, 36%); Anal. Calc. for $C_{49}H_{43}N_2OP_2Ir$: C, 63.27; H, 4.62; N, 3.01. Found: C, 63.11; H, 4.68; N, 3.05%. ^{1}H NMR: −19.44 (d of t, hydride, J_d = 6.6 Hz, J_t = 6.9 Hz); −20.20 (d of t, hydride, J_d = 6.6 Hz, J_t = 6.6 Hz); 2.21 (CH_3); 6.34 (t, H, *J* = 6.4 Hz); 6.48 (d, 2H, *J* = 8.1 Hz); 6.77 (d, 2H, *J* = 8.1 Hz); 7.13–7.53 (2PPh$_3$); 7.57 (d, H, *J* = 4.9 Hz); 7.71 (2H)*. Complex **2-H**: Yield: (35 mg, 39%); Anal. Calc. for $C_{48}H_{41}N_2OP_2Ir$: C, 62.39; H, 4.47; N, 3.05. Found: C, 63.55; H, 4.34; N, 3.07%. ^{1}H NMR: −19.39 (d of t, hydride J_d = 6.9 Hz, J_t = 6.6 Hz); −20.25 (d of t, hydride, J_d = 6.6 Hz, J_t = 6.6 Hz); 6.35 (t, H, *J* = 6.2 Hz); 6.67 (2H)*; 6.94 (d, 2H, *J* = 5.5 Hz); 7.12–7.4 (2PPh$_3$); 7.56 (d, H, *J* = 5.1 Hz); 7.74 (2H)*. Complex **2-Cl**: Yield: (35 mg, 37%); Anal. Calc. for $C_{48}H_{40}N_2OClP_2Ir$: C, 60.64; H, 4.21; N, 2.94. Found: C, 60.61; H, 4.25; N, 2.95%. ^{1}H NMR: −19.46 (d of t, hydride, J_d = 6.6 Hz, J_t = 6.6 Hz); −20.34 (d of t, hydride, J_d = 6.9 Hz, J_t = 6.9 Hz); 6.35 (t, H, *J* = 6.3 Hz); 6.60 (d, 2H, *J* = 8.8 Hz); 6.88 (d, 2H, *J* = 8.8 Hz); 7.12–7.46 (2PPh$_3$); 7.57 (d, H, *J* = 5.2 Hz); 7.73 (2H)*. Complex **2-NO$_2$**: Yield: (34 mg, 36%); Anal. Calc. for $C_{48}H_{40}N_3O_3P_2Ir$: C, 59.98; H, 4.16; N, 4.37. Found: C, 59.93; H, 4.22; N, 4.33%. ^{1}H NMR: −19.39 (d of t, hydride, J_d = 6.9 Hz, J_t = 6.6 Hz); −20.56 (d of t, hydride, J_d = 6.9 Hz, J_t = 6.9 Hz); 6.43 (t, H, *J* = 6.3 Hz); 7.12–7.44 (2PPh$_3$); 7.54 (3H)*; 7.63 (2H)*; 7.77 (2H)*.

Complexes **3** and **4**: To a solution of *N*-(1-naphthyl)picolinamide (**L^2**) (25 mg, 0.10 mmol) in warm ethanol (50 mL), triethylamine (10 mg, 0.10 mmol) was added followed by [Ir(PPh$_3$)$_3$Cl] (100 mg, 0.10 mmol). The mixture was refluxed for 24 h, whereby an orange solution was obtained. Evaporation of this solution afforded an orange solid, which was subjected to purification by thin layer chromatography on a silica plate. With 1:5 acetonitrile–benzene two orange bands separated, a thin light-orange band followed by a major deep orange band, both of which were extracted with acetonitrile. Evaporation of these extracts, respectively, gave complexes **3** and **4** as crystalline orange solids.

Complex **3**: Yield: (5 mg, 5%); Anal. Calc. for $C_{52}H_{40}N_2OP_2ClIr$: C, 62.57; H, 4.01; N, 2.80. Found: C, 62.73; H, 4.08; N, 2.79%. ^{1}H NMR: 6.57 (t, H, *J* = 7.7 Hz); 6.78 (2H)*; 6.90 (d, H, *J* = 4.7 Hz); 6.93–7.12 (2PPh$_3$); 7.55 (d, H, *J* = 6.5 Hz); 7.70 (t, H, *J* = 7.5 Hz); 7.91 (d, H, *J* = 7.8 Hz); 8.10 (d, H, *J* = 8.2 Hz). Complex **4**: Yield: (68 mg, 70%); Anal. Calc. for $C_{52}H_{41}N_2OP_2Ir$: C, 64.78; H, 4.25; N, 2.90. Found: C, 64.56; H, 4.28; N, 2.93%. ^{1}H NMR: −14.48 (t, hydride, *J* = 17.8 Hz); 6.37 (2H)*; 6.56 (d, *J* = 6.6 Hz, H); 6.82 (d, H, *J* = 7.9 Hz); 6.82 (2H)*; 6.99–7.34 (2PPh$_3$); 7.35 (d, H, *J* = 5.2 Hz); 7.42 (t, H, *J* = 7.7 Hz); 7.83 (d, H, *J* = 7.8 Hz); 8.27 (d, H, *J* = 6.8 Hz).

4.2. X-ray crystallography

Single crystals of **1-OCH$_3$** were obtained by slow evaporation of a solution of the complex in 1:1 dichloromethane-acetonitrile, and those of **2-Cl** and **3** were obtained similarly from acetonitrile solutions of the complexes. Selected crystal data and data collection parameters are given in Table 1. Data were collected on a Bruker SMART 1000 CCD diffractometer using graphite monochromated Mo Kα radiation (λ = 0.71073 Å). X-ray data reduction, structure solution and refinement were done using SHELXS-97 and SHELXL-97 programs [20]. The structures were solved by the direct methods.

Acknowledgements

The authors thank the referees for their constructive comments, which have been helpful in preparing the revised manuscript. Financial assistance received from the Department of Science and Technology [Grant No. SR/S1/IC-15/2004] is gratefully

acknowledged. Thanks are also due to the University Grants Commission, New Delhi [Grant No. F31-124/2005(SR)], for financial help.

Appendix A. Supplementary material

CCDC 672144, 672145 and 672146 contain the supplementary crystallographic data for this paper. These data can be obtained free of charge from The Cambridge Crystallographic Data Centre via www.ccdc.cam.ac.uk/data_request/cif. Supplementary data associated with this article can be found, in the online version, at doi:10.1016/j.jorganchem.2008.07.027.

References

[1] (a) C.E. Housecroft, Coord. Chem. Rev. 115 (1992) 163;
(b) C.E. Housecroft, Coord. Chem. Rev. 115 (1992) 191;
(c) C.E. Housecroft, Coord. Chem. Rev. A134 (1994) 307;
(d) C.E. Housecroft, Coord. Chem. Rev. 146 (1995) 235;
(e) C.E. Housecroft, Coord. Chem. Rev. 146 (1995) 269;
(f) C.E. Housecroft, Coord. Chem. Rev. 152 (1996) 107;
(g) C.E. Housecroft, Coord. Chem. Rev. 152 (1996) 141;
(h) M.J. Hannon, Coord. Chem. Rev 152 (1996) 393;
(i) M.C. Simpson, D.J.C. Hamilton, Coord.Chem. Rev. 155 (1996) 163;
(j) M.J. Hannon, Coord. Chem. Rev. 162 (1997) 477;
(k) A.M. Trezeciak, J.J. Ziolkowski, Coord. Chem. Rev. 190–192 (1999) 883;
(l) M.A. Esteruelas, L.A. Oro, Coord.Chem. Rev. 193–195 (1999) 557;
(m) I.M. Dixon, J.-P. Collin, J.-P. Sauvage, L. Flamigni, S. Encinas, F. Barigelletti, Chem. Soc. Rev. 385 (2000);
(n) J. Chen, R.J. Angelici, Coord. Chem. Rev. 206–207 (2000) 63;
(o) C. Slugovc, I. Padilla-Martnez, S. Sirol, E. Carmona, Coord. Chem. Rev. 213 (2001) 129;
(p) C.E. Webster, M.B. Hall, Coord. Chem. Rev. 238–239 (2003) 315;
(q) N. Pinault, D.W. Bruce, Coord. Chem. Rev. 241 (2003) 1;
(r) E. Baranoff, J.-P. Collin, L. Flamigni, J.-P. Sauvage, Chem. Soc. Rev. 147 (2004).
[2] (a) R. Acharyya, F. Basuli, R.Z. Wang, T.C.W. Mak, S. Bhattacharya, Inorg. Chem. 43 (2004) 704;
(b) S. Basu, S.M. Peng, G.H. Lee, S. Bhattacharya, Polyhedron 24 (2005) 157;
(c) S. Basu, I. Pal, R.J. Butcher, G. Rosair, S. Bhattacharya, J. Chem. Sci. 117 (2005) 167;
(d) R. Acharyya, F. Basuli, S.M. Peng, G.H. Lee, R.Z. Wang, T.C.W. Mak, S. Bhattacharya, J. Organomet. Chem. 690 (2005) 3908;
(e) S. Basu, R. Acharyya, W.S. Sheldrick, H.M. Figge, S. Bhattacharya, Struct. Chem. 18 (2007) 209.
[3] (a) H. Sigel, C.F. Naumann, B. Prijs, D.B. McCormick, M.C. Falk, Inorg. Chem. 16 (1977) 790;
(b) H. Sigel, Inorg. Chem. 14 (1975) 1535;
(c) M.F. El-Shazly, El-Dissowky, T. Salem, M. Osman, Inorg. Chim. Acta 40 (1980) 1;
(d) D.W. Margerum, Pure Appl. Chem. 55 (1983) 23;
(e) A.S. Borovik, T.M. Dewey, K.N. Raymond, Inorg. Chem. 32 (1993) 413;
(f) T.J. Collins, Acc. Chem. Res. 27 (1994) 279;
(g) M.J. Bartos, S.W. Gordon-Wylie, B.G. Fox, L.J. Wright, S.T. Weintraub, K.E. Kauffmann, E. Münck, K.L. Koskta, E.S. Uffelman, C.E.F. Rickard, K.R. Noon, T.J. Collins, Coord. Chem. Rev. 174 (1998) 361;
(h) A. White, X. Ding, J.C. vanderSpek, J.R. Murphy, D. Ringe, Nature 394 (1998) 502;
(i) E. Pohl, R.K. Holmes, W.G.J. Hol, J. Mol. Biol. 292 (1999) 653;
(j) B.M. Trost, C.B. Lee, J. Am. Chem. Soc. 123 (2001) 3671;
(k) M.D. Feese, B.P. Ingason, J. Goranson-Siekierke, R.K. Holmes, W.G.J. Hol, J. Biol. Chem. 276 (2001) 5959;
(l) T.J. Collins, Acc. Chem. Res. 35 (2002) 782;
(m) B.M. Trost, K. Dogra, I. Hachiya, T. Emura, D.L. Hughes, S. Krska, R.A. Reamer, M. Palucki, N. Yasuda, P.J. Reider, Angew. Chem. Int. Ed. 41 (2002) 1929;
(n) B.M. Trost, M. Crawley, J. Am. Chem. Soc. 124 (2002) 9328.
[4] M. Dasgupta, S. Bhattacharya, unpublished results.
[5] (a) P. Ford, D.E.P. Rudd, R.G. Gaunder, H. Taube, J. Am. Chem. Soc. 90 (1968) 1187;
(b) A.W. Zanella, P.C. Ford, Inorg. Chem. 14 (1975) 42;
(c) T. Matsubara, P.C. Ford, Inorg. Chem. 15 (1976) 1107;
(d) Y. Ilan, H. Taube, Inorg. Chem. 22 (1983) 1655;
(e) Y. Ilan, M. Kapon, Inorg. Chem. 25 (1986) 2350;
(f) H.Y. Huang, W.J. Chen, C.C. Yang, A. Yeh, Inorg. Chem. 30 (1991) 1862;
(g) M.H. Chou, C. Creutz, N. Sutin, Inorg. Chem. 31 (1992) 2318;
(h) M.H. Chou, B.S. Brunschwig, C. Creutz, N. Sutin, A. Yeh, R.C. Chang, C.-T. Lin, Inorg. Chem. 31 (1992) 5347;
(i) M.H. Chou, D.J. Szalda, C. Creutz, N. Sutin, Inorg. Chem. 33 (1994) 1674;
(j) S.M. Redmore, C.D.F. Rickard, S.J. Webb, L.J. Wright, Inorg. Chem. 36 (1997) 4743.
[6] B. Albert, D. Bray, J. Lewis, M. Raff, K. Roberts, J.D. Watson, Molecular Biology of the Cell, third ed., MacMillan, New York, 1994 (Chapter 3).
[7] T. Kojima, K. Hayashi, Y. Matsuda, Inorg. Chem. 43 (2004) 6793.
[8] (a) H. Sigel, R.B. Martin, Chem. Rev. 82 (1982) 385;
(b) H.E. Bryndza, W. Tam, Chem. Rev. 88 (1988) 1163;
(c) K. Severin, R. Bergs, W. Beck, Angew. Chem. Int. Ed. 37 (1998) 1634;
(d) J.R. Fulton, A.W. Holland, D.J. Fox, R.G. Bergman, Acc. Chem. Res. 35 (2002) 44.
[9] (a) D.M. Tellers, J.C.M. Ritter, R.G. Bergman, Inorg. Chem. 38 (1999) 4810;
(b) C. Bolm, T. Focken, G. Raabe, Tetrahedron Asymmetry 14 (2003) 1733;
(c) H.L. Milton, M.V. Wheatley, A.M.Z. Slawim, J.D. Woollin, Polyhedron 23 (2004) 3211.
[10] (a) S.K. Burley, G.A. Petsko, Science 229 (1985) 23;
(b) H.C. Weiss, D. Blaser, R. Boese, B.M. Doughan, M.M. Haley, Chem. Commun. (1997) 1703;
(c) N.N.L. Madhavi, A.K. Katz, H.L. Carrell, A. Nangia, G.R. Desiraju, Chem. Commun. (1997) 1953;
(d) S.K. Burley, G.A. Petsko, Adv. Protein Chem. 39 (1988) 125;
(e) M. Nishio, M. Hirota, Y. Umezawa, The CH···π Interactions (Evidence, Nature and Consequences), Wiley–VCH, New York, 1998;
(f) Y. Umezawa, S. Tsuboyama, K. Honda, J. Uzawa, M. Nishio, Bull. Chem. Soc. Jpn. 71 (1998) 1207;
(g) G.R. Desiraju, T. Steiner, The Weak hydrogen Bond (IUCr Monograph on Crystallography 9), Oxford Science Publishing (1999);
(h) M.J. Hannon, C.L. Painting, N.W. Alcock, Chem. Commun. (1999) 2033;
(i) B.J. Mcnelis, L.C. Nathan, C.J. Clark, J. Chem. Soc. Dalton Trans. (1999) 1831;
(j) K. Biradha, C. Seward, M.J. Zaworotko, Angew. Chem. Int. Ed. 38 (1999) 492;
(k) M.J. Calhorda, Chem. Commun. 801 (2000);
(l) C. Janiak, S. Temizdemir, S. Dechert, Inorg. Chem. Commun. 3 (2000) 271;
(m) C. Janiak, S. Temizdemir, S. Dechert, W. Deck, F. Girgsdies, J. Heinze, M.J. Kolm, T.G. Scarmann, O.M. Zipffel, Eur. J. Inorg. Chem. (2000) 1229.
[11] (a) C.S. Yi, S.Y. Yun, I.A. Guzei, Organometallics 23 (2004) 5392;
(b) T. Li, R. Churlaud, A.J. Lough, K. Abdur-Rashid, R.H. Morris, Organometallics 23 (2004) 6239;
(c) R. CelenligilCetin, L.A. Watson, C. Guo, B.M. Foxman, O.V. Ozerov, Organometallics 24 (2005) 186;
(d) J.W. Diluzio, L. Vaska, J. Am. Chem. Soc. 83 (1961) 1262.
[12] Under ambient condition it takes approximately 5 h for 50% conversion of a **1-R** complex to the corresponding **2-R** complex.
[13] The evolved hydrogen could not be detected experimentally.
[14] C. Mealli, D.M. Proserpio, J. Chem. Educ. 67 (1990) 399.
[15] In the $R = NO_2$ complexes, the lowest unoccupied molecular orbital (LUMO) has more than 90% contribution from the amide ligand, but is concentrated largely on the NO_2 group.
[16] A little dichloromethane was necessary to take the complex into solution. Addition of large excess of acetonitrile was necessary to record the redox responses in proper shape.
[17] S. Dutta, S. Pal, P.K. Bhattacharya, Polyhedron 18 (1999) 2157.
[18] (a) D.T. Sawyer, J.L. Roberts Jr., Experimental Electrochemistry for Chemists, Wiley, New York, 1974;
(b) M. Walter, L. Ramaley, Anal. Chem. 45 (1973) 165.
[19] Chemical shifts are given in ppm and multiplicity of the signals along with the associated coupling constants (*J* in Hz) are given in parentheses. Overlapping signals are marked with an asterisk.
[20] G.M. Sheldrick, SHELXS-97 and SHELXL-97, Fortran programs for crystal structure solution and refinement, University of Gottingen, Gottingen, Germany, 1997.